

RESEARCH ARTICLE | MAY 03 2023

Theoretical upper limits of the thermal conductivity of Si_3N_4



Hao Zhou ; Tianli Feng



Appl. Phys. Lett. 122, 182203 (2023)

<https://doi.org/10.1063/5.0149298>



CrossMark

Lake Shore
CRYOTRONICS

CryoComplete

A total solution for low-temperature characterization

[Learn more >](#)

The advertisement features the Lake Shore CRYOTRONICS logo and the CryoComplete product name. It includes a photograph of the CryoComplete system, which consists of a computer monitor displaying the CryoComplete software interface, a control unit, and a cryogenic probe. The background is a light blue gradient.

Theoretical upper limits of the thermal conductivity of Si_3N_4

Cite as: Appl. Phys. Lett. **122**, 182203 (2023); doi: [10.1063/5.0149298](https://doi.org/10.1063/5.0149298)

Submitted: 5 March 2023 · Accepted: 21 April 2023 ·

Published Online: 3 May 2023



View Online



Export Citation



CrossMark

Hao Zhou  and Tianli Feng^{a)} 

AFFILIATIONS

Department of Mechanical Engineering, University of Utah, Salt Lake City, Utah 84112, USA

^{a)} Author to whom correspondence should be addressed: tianli.feng@utah.edu

ABSTRACT

Silicon nitride (Si_3N_4) is a promising substrate for high-power electronics due to its superior mechanical properties and potential outstanding thermal conductivity (κ). As experiments keep pushing the upper limit of κ of Si_3N_4 , it is believed that it can reach 450 W/mK, similar to SiC, based on classical models and molecular dynamics simulations. In this work, we reveal from first principles that the theoretical κ upper limits of β - Si_3N_4 are only 169 and 57 W/mK along the c and a axes at room temperature, respectively. Those of α - Si_3N_4 are about 116 and 87 W/mK, respectively. The predicted temperature-dependent κ matches well with the highest available experimental data, which supports the accuracy of our calculations, and suggests that the κ upper limit of Si_3N_4 has already been reached in the experiment. Compared to other promising semiconductors (e.g., SiC, AlN, and GaN), Si_3N_4 has a much lower κ than expected even though the chemical bonding and mechanical strengths are close or even stronger. We find the underlying reason is that Si_3N_4 has much lower phonon lifetimes and mean free paths ($<0.5 \mu\text{m}$) due to the larger three-phonon scattering phase space and stronger anharmonicity. Interestingly, we find that the larger unit cell (with more basis atoms) that leads to a smaller fraction of acoustic phonons is not the reason for lower κ . Grain size-dependent κ indicates that the grain boundary scattering plays a negligible role in most experimental samples. This work clarifies the theoretical κ upper limits of Si_3N_4 and can guide experimental research.

Published under an exclusive license by AIP Publishing. <https://doi.org/10.1063/5.0149298>

Thermal management of electronic devices plays a crucial role in normal operation where high temperature can degrade the performance and even destroy the devices, especially for highly integrated, high-power density, and miniaturized devices.^{1,2} An excellent candidate material used for thermal management should have both high thermal conductivity and mechanical strength to prevent devices from overheating and fracture.³ Silicon nitride (Si_3N_4) has received significant attention in this area owing to its superior properties. Because of the strong Si-N bond,⁴ Si_3N_4 ceramics exhibit excellent mechanical properties such as high strength at room and elevated temperatures and high hardness, which should lead to potential high thermal conductivity. In addition, Si_3N_4 possesses low thermal expansion, low density, and low dielectric constant.^{5–7} All these outstanding properties qualify Si_3N_4 as a promising substrate candidate for high-power electronic devices.

There are three typical crystallographic structures of Si_3N_4 , namely, α -, β -, and γ - Si_3N_4 .⁸ Among them, the γ phase is cubic, made through high temperature and high pressure, while the other two are more thermodynamically stable at room temperature with a hexagonal lattice.⁹ β - Si_3N_4 is more stable at high temperatures and is the most

commonly seen phase in applications. The α phase changes to β at high temperatures above 1300 °C.¹⁰ While the mechanical properties of Si_3N_4 are guaranteed by the strong bonding, the thermal conductivities of α and β phase have not been well studied yet. The theoretical study of the thermal conductivities of Si_3N_4 is very limited. In 1995, Haggerty and Lightfoot predicted the intrinsic thermal conductivity of β - Si_3N_4 to be 200 to 320 W/mK at room temperature based on Slack's relation.¹¹ In 2002, Hirosaki *et al.* revisited the theoretical values and predicted 170 and 450 W/mK along the a and c axes, respectively, by using molecular dynamics (MD) simulations with a classical potential.¹⁰ They also reported the thermal conductivities of the α phase as 105 and 225 W/mK along the a and c axes, respectively. However, all these works were based on empirical models, which may cause large mispredictions. For example, Slack's relation has many fitting parameters, and the choice of those parameters is arbitrary. Classical potential in MD simulations can give large errors for thermal conductivity as well. No first principles prediction has been carried out yet to unveil the intrinsic thermal conductivities of α - and β - Si_3N_4 . Therefore, there is an urgency to accurately predict the theoretical upper limit of thermal conductivities to guide experimental efforts.

Driven by the literature's theoretical predictions, experiments have been continuously pursuing the upper limit of thermal conductivity of β - Si_3N_4 , which is believed to be 200–450 W/mK, for more than two decades. In 1996, Hirosaki *et al.* obtained β - Si_3N_4 with a thermal conductivity of 120 W/mK by the addition of 1 mol. % of Y_2O_3 - Nd_2O_3 and sintering at 2000 °C.¹² They found that a higher sintering temperature can increase the thermal conductivity resulting from grain growth. In the same year, Hirao *et al.* reported a similar value of 122 W/mK for β - Si_3N_4 fabricated by tape casting.¹³ Their samples exhibited a high anisotropy, which was attributed to the orientation of elongated grains. The thermal conductivity perpendicular to the stacking direction was measured to be around 60 W/mK. In 1999, Watari *et al.* increased the thermal conductivity of β - Si_3N_4 parallel to the casting direction to 155 W/mK by high-temperature firing and proper seeds addition,¹⁴ though thermal conductivity along the other direction was still low, which was only 52 W/mK. In the same year, Li *et al.* enabled the measurement of a single β - Si_3N_4 grain and obtained 69 and 180 W/mK along the *a* and *c* axes, respectively.¹⁵ They also indicated that anisotropy is intrinsic. Later, an isotropic thermal conductivity (149 W/mK) of β - Si_3N_4 was realized by Furuya *et al.* in 2002 by combining high-quality seed crystals with the suitable additive system to promote grain growth.¹⁶ Afterward, β - Si_3N_4 produced by another method, namely, sintered reaction-bonding, which can provide lower cost and reduce the lattice oxygen, was investigated by Zhu, Zhou, and coauthors.^{17–22} The highest thermal conductivity achieved was 177 W/mK. Moreover, many other experimental attempts have been made to promote the thermal conductivity of β - Si_3N_4 until today, and experimentalists assume the theoretical upper limit is 200–450 W/mK.^{23–31} The reason the measured values have not reached this limit was believed to be the existence of the secondary phase (mainly lattice oxygen), grain boundary, and imperfections (vacancies, dislocations, etc.). However, it remains a question whether it is because the theoretical predictions are wrong.

In this Letter, we unveil the intrinsic thermal conductivities of α - and β - Si_3N_4 by solving the phonon Boltzmann transport equation (BTE) based on first principles. The thermal conductivities of Si_3N_4 obtained are compared with literature data for Si_3N_4 and other promising ceramics. To understand the difference between them, we compare their phonon dispersions, velocities, lifetimes, and mean free paths (MFPs). The impacts of grain size on thermal conductivities were also explored.

All the first principles calculations were performed by using the Vienna *ab initio* simulation package (VASP)³² with the projected augmented wave (PAW)³³ method based on the density functional theory (DFT). Local density approximation (LDA)³⁴ was chosen as the exchange-correlation functional. The plane wave energy cutoff was selected as 500 eV. During the structure optimization process, atomic positions and the lattice constants were both allowed to be relaxed until the maximal residual energy was smaller than 10^{-8} eV. The force convergence threshold was 10^{-7} eV/Å. K-meshes of α - and β - Si_3N_4 are $6 \times 6 \times 9$ and $8 \times 8 \times 16$, respectively, to keep the consistency since different sizes of supercells were made in the force constant calculations. The obtained lattice constants for α - Si_3N_4 are 7.724 and 5.598 Å along *a* and *c* axes, respectively. For β - Si_3N_4 , the lattice constants are 7.578 and 2.892 Å along *a* and *c* axes, respectively. All the results agree well with experimental data.^{35,36} In the calculation of harmonic and anharmonic force constant using Phonopy³⁷ and

Thirdorder,³⁸ the supercell size was selected as $2 \times 2 \times 3$ (336 atoms) with a $3 \times 3 \times 3$ k-mesh for α - Si_3N_4 and $2 \times 2 \times 4$ (224 atoms) with a $4 \times 4 \times 4$ k-mesh for the β phase. The energy convergence threshold is 10^{-8} eV. The first principles calculation is computationally heavy due to the large unit cells. The non-analytical correction³⁹ that splits LO and TO phonons at the Γ point was considered in the phonon dispersion calculations. Up to the 6th nearest neighbor of atoms was included for both phases in anharmonic force constant extraction. We do not consider four-phonon scattering since there is no acoustic-optical bandgap, and we focus on low temperatures. The results compared to the experiment also indicate that four-phonon scattering is not important.

The temperature-dependent thermal conductivity, phonon MFP-cumulative thermal conductivity, group velocity, scattering rate, and Grüneisen parameters were calculated by ShengBTE³⁸ using a $10 \times 10 \times 10$ phonon **q**-mesh for α - Si_3N_4 and a $12 \times 12 \times 12$ phonon **q**-mesh for β - Si_3N_4 . The broadening factor was set to 0.1. The calculation convergence regarding **q**-mesh and broadening factor was tested. Natural isotope-phonon scattering was included. Grain size impact is included by including a phonon-boundary scattering rate.⁴⁰

The phonon dispersions and densities of states of α - and β - Si_3N_4 are shown in Fig. 1. Both phases have high frequencies up to around 34 THz, indicating a strong bonding. Both phases have many atoms, i.e., 28 for α and 14 for β , in the primitive cell. As a result, the three acoustic phonon modes only occupy 3.57% and 7.14% of the total phonon modes for the α and β phases, respectively. Both phases have acoustic phonons up to around 7 THz, which was contributed by both Si and N atoms evenly based on the projected DOS.

The calculated temperature-dependent thermal conductivities of β - Si_3N_4 and corresponding experimental data from the literature are shown in Fig. 2(a). The two curves represent our first principles results for the *a* and *c* axes, and the points are experimental data from the literature. Thermal conductivity along the *c* axis is larger than that along the *a* axis, which suggests an intrinsic anisotropy in the hexagonal lattice. Some of the experimental data reported the anisotropy of thermal conductivities, designated by squares and circles symbols with squares indicating the higher values,^{13–15,41,42} while the others only provided one single value without mentioning any details about the orientation-dependent information, designated by cross signs.^{12,16,18,22,25,28–30,43}

“//” and “ \perp ” indicate parallel or perpendicular to tape casting direction for Watari's¹⁴ and Hirao's¹³ results and hot-pressing direction for Kitayama's⁴¹ and Liang's⁴² results since they adopted different methods to produce Si_3N_4 samples. Based on our DFT calculations, the intrinsic thermal conductivities of β - Si_3N_4 at room temperature are 169 and 57 W/mK along the *c* and *a* axes, respectively, which are much smaller than Haggerty and Lightfoot's prediction based on Slack's relation¹¹ and Hirosaki's classical MD simulation.¹⁰ This indicates that their estimations may mislead the audience.

As can be seen from the figure, at room temperature, almost all the experimental values are between our predicted thermal conductivities along two axes, and some of them are very close to the intrinsic value along the *c* axis. For those experiments reporting anisotropic thermal conductivities along two perpendicular directions, some of them^{14,15} reached our predicted value (upper limit) along the *c* axis, and the others did not.^{13,41} Note that these experiments did not explicitly measure the *a* and *c* axes but two preferred perpendicular directions, which are not necessarily aligned along the two axes. In other studies

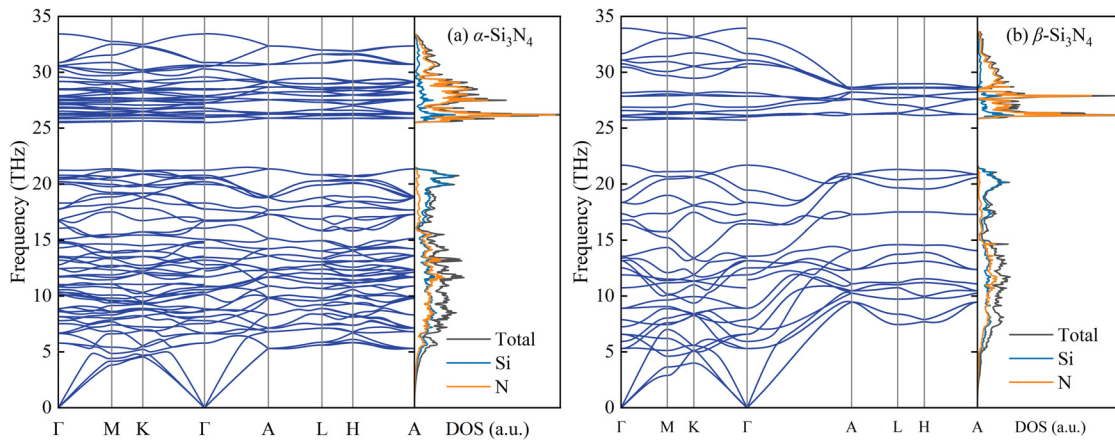


FIG. 1. Phonon dispersions and densities of states (DOS) of (a) α - Si_3N_4 and (b) β - Si_3N_4 .

where there is only one single thermal conductivity reported, it can be understood as either the isotropic value due to disordered grains or just the thermal conductivity along a certain direction that is not specified. Based on our estimation, the upper and lower limits of isotropic thermal conductivities of β - Si_3N_4 are $(\kappa_a + \kappa_b + \kappa_c)/3 = 94.3 \text{ W/mK}$ and $3/(\frac{1}{\kappa_a} + \frac{1}{\kappa_b} + \frac{1}{\kappa_c}) = 73.16 \text{ W/mK}$, respectively. This means most of the values^{18,22,25,28,30} reported should be along a certain direction since they are even larger than 100 W/mK. It should also be pointed out that the reported highest isotropic thermal conductivities (149 W/mK)¹⁶ may not be reliable based on the aforementioned estimation. Among these experimental results, the highest one was achieved by Zhou *et al.*²² in 2015 with a thermal conductivity of 177 W/mK, which is close to our prediction. The thermal conductivity reported by Li *et al.*¹⁵ is slightly higher than the value of Zhou *et al.*,²² but they just measured the thermal conductivity in a single grain instead of the whole material. Their in-grain intrinsic thermal conductivity value further validates our prediction.

Regarding the temperature-dependent thermal conductivity, it can be seen from the figure that our predicted values agree well with experimental data of Watari *et al.*¹⁴ throughout the temperature range, which is a clear evidence that our prediction is reliable. If grain boundary or defects play a role in the experimental sample, its temperature dependence should be altered and be different from the $1/T$ trend predicted by first principles.⁴⁴⁻⁴⁷ In addition, their perpendicular thermal conductivities are slightly larger than our simulated value along the a axis. This could be their reported value mistake since they reported 52 W/mK at room temperature but plotted as 68 W/mK in their figure. Note that 52 W/mK agrees with our prediction. We further checked the off-diagonal inter-band contribution since it can bend up the temperature-dependency trend of thermal conductivity based on the Wigner formulation.⁴⁸ However, it was found that the contribution of the off-diagonal term is only 0.5 W/mK at 1000 K, much smaller than the intrinsic phonon-gas value. Moreover, it should be noted that DFT calculation cannot be absolutely accurate, since the use of different pseudopotentials, number of nearest neighbors, energy cutoff, etc., will

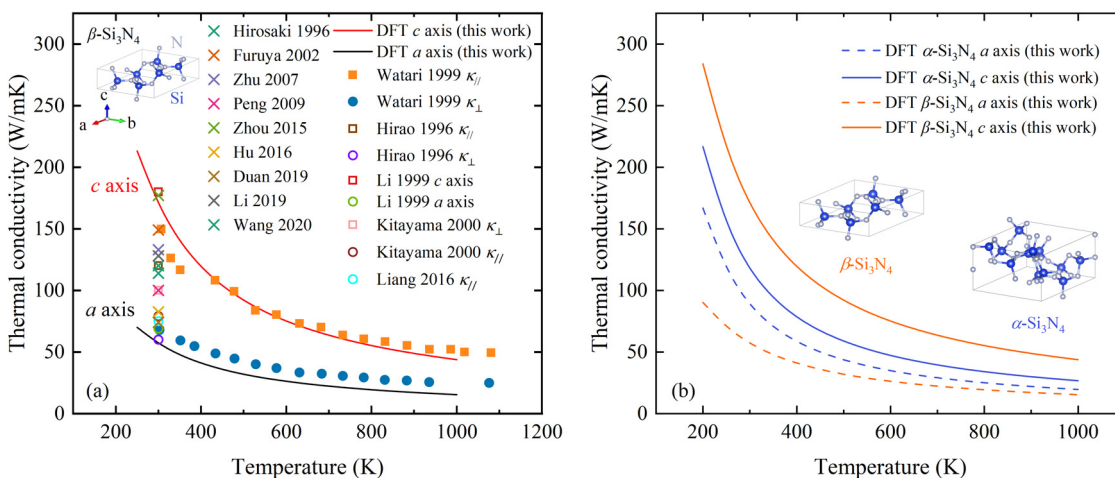


FIG. 2. (a) Temperature-dependent thermal conductivities of β - Si_3N_4 from first principles compared to experimental data from the literature; (b) predicted temperature-dependent thermal conductivities of α - Si_3N_4 and β - Si_3N_4 from first principles.

Downloaded from http://pubs.aip.org/apl/article-pdf/doi/10.1063/5.0149298/182203_1_5.0149298.pdf

all give slight differences. However, considering the good agreement between the experimental results and our predictions, it can be concluded that our prediction of the thermal conductivity of β -Si₃N₄ is convincing, and the experimental efforts have already reached the upper limit of the thermal conductivities of β -Si₃N₄. The hypothesis in the literature that the secondary phase (mainly lattice oxygen), grain boundary, and imperfections (vacancies, dislocations, etc.) degraded the thermal conductivity is likely not true. The existence of those factors should play insignificant role on the thermal conductivity of experimental samples.

Since the α phase is also commonly seen at room temperature, we have also predicted its thermal conductivity, as shown in Fig. 2(b). Thermal conductivities of α -Si₃N₄ were found to be 87 and 116 W/mK along the a and c axes at room temperature, respectively. As the temperature goes up, thermal conductivities of both phases decrease. Overall, β -Si₃N₄ owns the highest thermal conductivity along the c axis but lowest along the a axis. α -Si₃N₄ shows less significant anisotropy compared with the β phase.

Since Si₃N₄ and SiC have similar Debye temperature, atomic bonding strength, mechanical strength, average atomic volume, and average atomic mass, based on Slack's relation, they should have comparable thermal conductivities.¹¹ Here, we compare the intrinsic thermal conductivities of Si₃N₄, 3C-SiC,⁴⁹ 4H-SiC,⁵⁰ 6H-SiC,⁵⁰ AlN,⁵¹ and GaN,⁵⁰ which are also promising semiconductors or substrates and have well-agreed thermal conductivities values from first principles prediction and experiment. As shown in Fig. 3, 3C-SiC possesses the highest thermal conductivity, which is 511 W/mK at room temperature. However, the intrinsic thermal conductivities of the three polymorphs of Si₃N₄ are much smaller than SiC and are the lowest among all the materials. This may suggest that Si₃N₄ may not be the best candidate for substrates in terms of thermal transport.

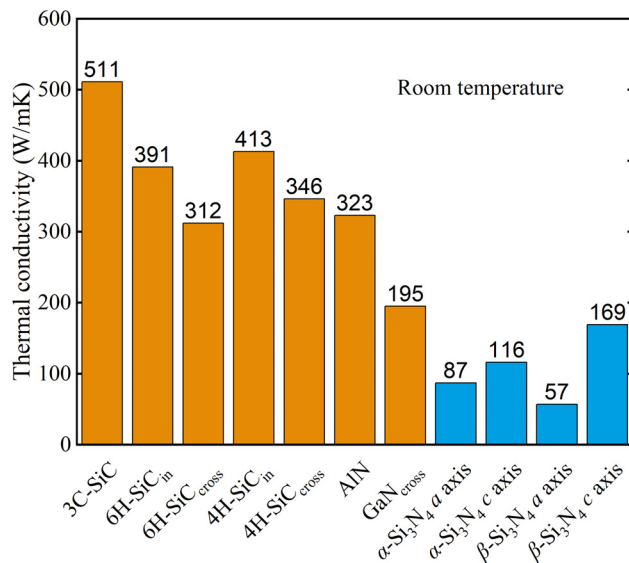


FIG. 3. Comparison of the thermal conductivities between Si₃N₄ and 3C-SiC,⁴⁹ 6H-SiC,⁵⁰ 4H-SiC,⁵⁰ AlN,⁵¹ and GaN⁵⁰ at room temperature. AlN and GaN also have anisotropy but are not significant and not shown here.

To find out the reason why thermal conductivities of β -Si₃N₄ are much lower than other materials,⁴⁹ we compare its phonon MFP-cumulative thermal conductivities, phonon group velocities, lifetimes, three-phonon scattering phase space, and Grüneisen parameters, with 3C-SiC at room temperature, as shown in Fig. 4. We find that β -Si₃N₄ has much shorter MFP, slower group velocities, and shorter phonon lifetimes. For example, the medium MFP of β -Si₃N₄ along a and c axes is both around 80 nm, while that of 3C-SiC is 500 nm. The averaged group velocity of β -Si₃N₄ is much lower than that of 3C-SiC, even though they share the similar sound velocity (phonon velocity at the low-frequency limit). The shorter lifetime of β -Si₃N₄ than 3C-SiC originates from the larger phonon-phonon scattering phase space and stronger anharmonicity as shown in Figs. 4(d) and 4(e). However, it remains a question why the anharmonicity of Si₃N₄ is significant while having strong interatomic bonding. First, Young's modulus of Si₃N₄ (320 GPa⁵²) is not as high as that of SiC (425 GPa⁵³). This indicates the bond of Si₃N₄ is not as strong as that of SiC. Second, anharmonicity, although somewhat positively correlated with bonding strength, is not determined solely by bonding strength. The potential well can deviate from the parabolic shape in various ways, representing various forms of anharmonicity, even for the same spring constant (or strength of bonding).

It is usually believed that complex crystals have smaller thermal conductivity due to the smaller fraction of acoustic phonon modes, given the larger number of atoms in the unit cell. For example, the primitive cells of β -Si₃N₄ and 3C-SiC contain 14 and 2 atoms, respectively. As a result, the three acoustic modes only take 7.14% portion of the total number of phonon modes of Si₃N₄ but 50% of 3C-SiC. The acoustic phonon frequency range of Si₃N₄ is only 0–8 THz but is 0–19 THz for 3C-SiC.⁴⁹ However, after checking the frequency-cumulative thermal of the two materials conductivity as shown in Fig. 4(f), a contradictory trend is found: the two materials have nearly identical frequency dependent thermal conductivity contribution. This finding shows that it is not true that optical phonons' contribution is not negligible and is comparable to acoustic phonons of Si₃N₄. Actually, the optical phonons contribute to 55.07% and 62.26% of the thermal conductivity in Si₃N₄ along a and c axes, respectively. It indicates that the larger unit cell (with more basis atoms) that leads to smaller fraction of acoustic phonons is not the reason for lower thermal conductivity. This conclusion is in agreement with a recent study by Dai and Tian,⁵⁴ who revealed that thermal conductivities of B₆O (i.e., α -B₆O and β -B₆O) could be as high as 200–300 W/mK even though they have complex crystal structures. It is also consistent with the fact that the different polytypes of a material have similar thermal conductivity, even though their unit cell sizes differ by several times; for example, thermal conductivities of SiC (i.e., 3C-SiC, 4H-SiC, and 6H-SiC) are all around 400–500 W/mK. Here, the two polytypes of Si₃N₄ also have similar thermal conductivity of 80–90 W/mK (after averaging the anisotropy) even though their unit cell size differs significantly.

Since experimental samples often have grain boundaries, it is necessary to predict the impact of grain sizes on thermal transport. As shown in Fig. 5, the thermal conductivity of a grain can reach 80% of bulk thermal conductivity at the size of 0.2 μ m for the a axis and 0.32 μ m for the c axis. It is safe to conclude that once the grain size is larger than 2 μ m, grain size plays a little role in the measured thermal conductivities. Since the grain size of most of the experimental samples

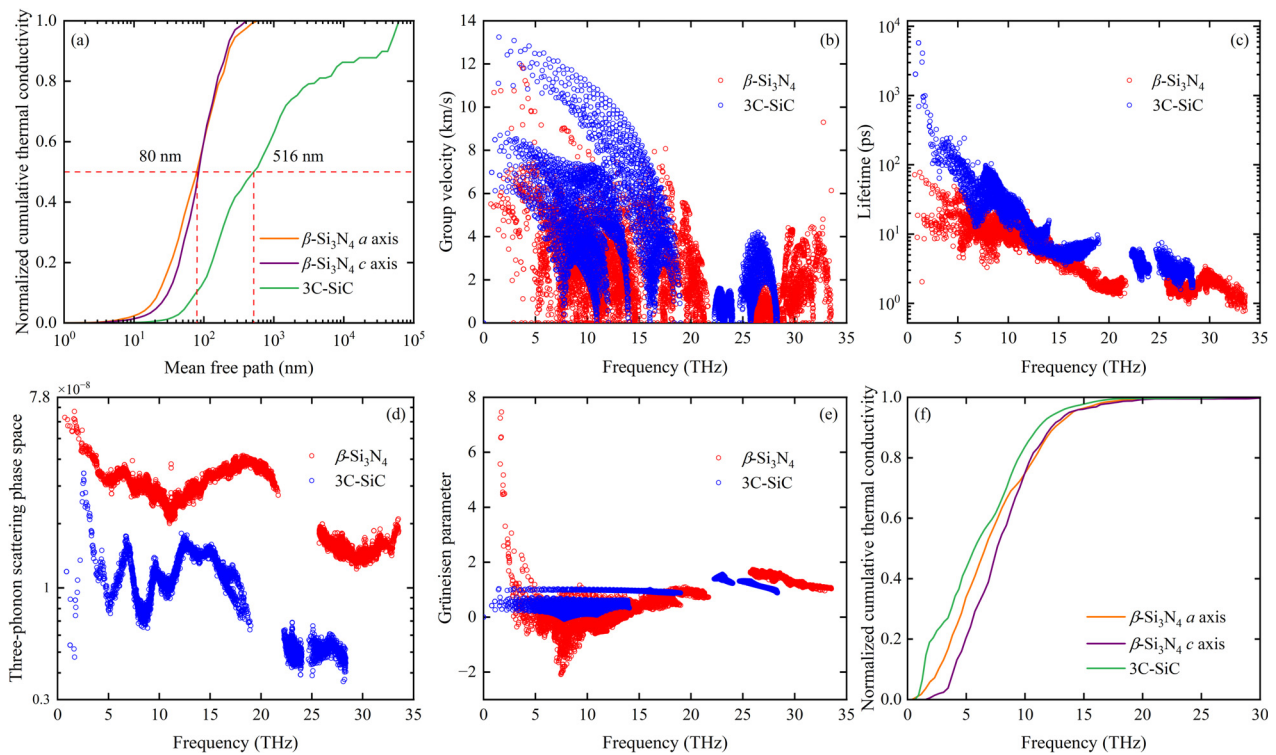


FIG. 4. Comparison between β -Si₃N₄ and 3C-SiC⁴⁹ at room temperature for (a) normalized MFP-cumulative thermal conductivities, (b) phonon group velocities, (c) phonon lifetimes, (d) three-phonon scattering phase space, (e) Grüneisen parameters, and (f) normalized frequency-cumulative thermal conductivities.

is large enough,^{15,22,23,27} the impact of grain size should not be a concern in the experiments.

To summarize, we have revisited the theoretical thermal conductivity upper limit of α - and β -Si₃N₄ by using first principles. We find

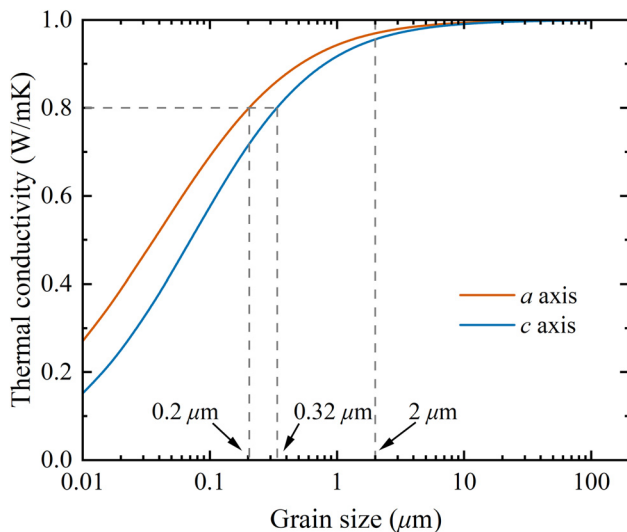


FIG. 5. Normalized grain size-dependent thermal conductivity of β -Si₃N₄ along a and c axes.

that they are much smaller than believed. The thermal conductivities of β -Si₃N₄ at room temperature are 169 and 57 W/mK along the c and a axes, respectively. For the α phase, they are 116 and 87 W/mK, respectively. The previous high predictions based on empirical models are not reliable. The experimental efforts in the literature have already reached the upper limit of the β -Si₃N₄. The large volume for three-phonon scattering and anharmonicity of β -Si₃N₄ are responsible for the lower thermal conductivity of Si₃N₄ compared to other similar ceramics such as SiC, AlN, and GaN. Grain size-dependent thermal conductivity results suggest that the impact of grain size is negligible in most experiments as their grains are usually larger than 2 μ m. We expect this work to be crucial in semiconductors development.

This work was supported by the National Science Foundation (NSF) (Award No. CBET 2212830). The computation used the resources from the Center for High Performance Computing (CHPC) at the University of Utah, the Advanced Cyberinfrastructure Coordination Ecosystem: Services & Support (ACCESS) of NSF, and the National Energy Research Scientific Computing Center (NERSC), a DOE Office of Science User Facility under Contract No. DE-AC02-05CH11231 and Award No. BES-ERCAP0022132.

AUTHOR DECLARATIONS

Conflict of Interest

The authors have no conflicts to disclose.

Author Contributions

Hao Zhou: Formal analysis (lead); Investigation (lead); Writing – original draft (lead). **Tianli Feng:** Conceptualization (lead); Formal analysis (supporting); Funding acquisition (lead); Investigation (supporting); Supervision (lead); Writing – review & editing (lead).

DATA AVAILABILITY

The data that support the findings of this study are available from the corresponding author upon reasonable request.

REFERENCES

- ¹H. Okumura, *Jpn. J. Appl. Phys., Part 1* **45**(10R), 7565 (2006).
- ²S. P. Gurrum, S. K. Suman, Y. K. Joshi, and A. G. Fedorov, *IEEE Trans. Device Mater. Reliab.* **4**(4), 709–714 (2004).
- ³D. Graovac, A. Christmann, and M. Munzer, in *8th International Conference on Power Electronics - ECCE Asia* (IEEE, 2011), pp. 1666–1673.
- ⁴F. Gao, J. He, E. Wu, S. Liu, D. Yu, D. Li, S. Zhang, and Y. Tian, *Phys. Rev. Lett.* **91**(1), 015502 (2003).
- ⁵R. N. Katz, *MRS Proc.* **287**, 197 (1992).
- ⁶F. L. Riley, *J. Am. Ceram. Soc.* **83**(2), 245–265 (2004).
- ⁷H. Klemm, *J. Am. Ceram. Soc.* **93**(6), 1501–1522 (2010).
- ⁸A. Kuwabara, K. Matsunaga, and I. Tanaka, *Phys. Rev. B* **78**(6), 064104 (2008).
- ⁹J. Liu, S. Ju, N. Nishiyama, and S. Junichiro, *Phys. Rev. B* **100**(6), 064303 (2019).
- ¹⁰N. Hirosaki, S. Ogata, C. Kocer, H. Kitagawa, and Y. Nakamura, *Phys. Rev. B* **65**(13), 134110 (2002).
- ¹¹J. S. Haggerty and A. Lightfoot, in *Ceramic Engineering & Science Proceedings* (ACM, 1995), p. 475.
- ¹²N. Hirosaki, Y. Okamoto, M. Ando, F. Munakata, and Y. Akimune, *J. Am. Ceram. Soc.* **79**(11), 2878–2882 (1996).
- ¹³K. Hirao, K. Watari, M. E. Brito, M. Toriyama, and S. Kanzaki, *J. Am. Ceram. Soc.* **79**(9), 2485–2488 (1996).
- ¹⁴K. Watari, K. Hirao, M. E. Brito, M. Toriyama, and S. Kanzaki, *J. Mater. Res.* **14**(4), 1538–1541 (1999).
- ¹⁵B. Li, L. Pottier, J. P. Roger, D. Fournier, K. Watari, and K. Hirao, *J. Eur. Ceram. Soc.* **19**(8), 1631–1639 (1999).
- ¹⁶K. Furuya, F. Munakata, K. Matsuo, Y. Akimune, J. Ye, and A. Okada, *J. Therm. Anal. Calorim.* **69**(3), 873–879 (2002).
- ¹⁷X. Zhu, Y. Zhou, K. Hirao, and Z. Lenčič, *J. Am. Ceram. Soc.* **89**(11), 3331–3339 (2006).
- ¹⁸X. Zhu, Y. Zhou, K. Hirao, and Z. Lenčič, *J. Am. Ceram. Soc.* **90**(6), 1684–1692 (2007).
- ¹⁹Y. Zhou, X. Zhu, K. Hirao, and Z. Lences, *Int. J. Appl. Ceram. Technol.* **5**(2), 119–126 (2008).
- ²⁰X. W. Zhu, Y. Sakka, Y. Zhou, and K. Hirao, *J. Ceram. Soc. Jpn.* **116**(1354), 706–711 (2008).
- ²¹Y. Zhou, H. Hyuga, D. Kusano, Y. I. Yoshizawa, and K. Hirao, *Adv. Mater.* **23**(39), 4563–4567 (2011).
- ²²Y. Zhou, H. Hyuga, D. Kusano, Y. I. Yoshizawa, T. Ohji, and K. Hirao, *J. Asian Ceram. Soc.* **3**(3), 221–229 (2015).
- ²³W. Wang, D. Yao, H. Liang, Y. Xia, K. Zuo, J. Yin, and Y. P. Zeng, *J. Eur. Ceram. Soc.* **41**(2), 1735–1738 (2021).
- ²⁴Y. Wang, X. Li, H. Wu, B. Jia, D. Zhang, Y. Zhang, Z. Zhang, J. Tian, M. L. Qin, and X. Qu, “Thermal conductivity of Si₃N₄ ceramics fabricated from carbothermal-reduction-derived powder,” <https://www.researchsquare.com/article/rs-910628/v1>.
- ²⁵W. Wang, D. Yao, H. Chen, Y. Xia, K. Zuo, J. Yin, H. Liang, and Y. Zeng, *J. Am. Ceram. Soc.* **103**(3), 2090–2100 (2020).
- ²⁶F. Hu, Z. P. Xie, J. Zhang, Z. L. Hu, and D. An, *Rare Met.* **39**(5), 463–478 (2020).
- ²⁷H. Liang, W. Wang, K. Zuo, Y. Xia, D. Yao, J. Yin, and Y. Zeng, *Ceram. Int.* **46**(11), 17776–17783 (2020).
- ²⁸Y. Li, H. N. Kim, H. Wu, M. J. Kim, J. W. Ko, Y. J. Park, Z. Huang, and H. D. Kim, *J. Eur. Ceram. Soc.* **39**(2–3), 157–164 (2019).
- ²⁹F. Hu, L. Zhao, and Z. P. Xie, *J. Ceram. Sci. Technol.* **7**(4), 423–428 (2016).
- ³⁰G. H. Peng, M. Liang, Z. H. Liang, Q. Y. Li, W. L. Li, and Q. Liu, *J. Am. Ceram. Soc.* **92**(9), 2122–2124 (2009).
- ³¹S. Liao, L. Zhou, K. Yin, J. Wang, and C. Jiang, *Mater. Rep.* **34**(11), 21105–21114 (2020).
- ³²G. Kresse and J. Furthmüller, *Phys. Rev. B* **54**(16), 11169–11186 (1996).
- ³³P. E. Blöchl, *Phys. Rev. B* **50**(24), 17953–17979 (1994).
- ³⁴J. P. Perdew and A. Zunger, *Phys. Rev. B* **23**(10), 5048–5079 (1981).
- ³⁵D. du Boulay, N. Ishizawa, T. Atake, V. Streltsov, K. Furuya, and F. Munakata, *Acta Crystallogr. B* **60**(4), 388–405 (2004).
- ³⁶H. Toraya, *J. Appl. Crystallogr.* **33**(1), 95–102 (2000).
- ³⁷A. Togo, F. Oba, and I. Tanaka, *Phys. Rev. B* **78**(13), 134106 (2008).
- ³⁸W. Li, J. Carrete, N. A. Katcho, and N. Mingo, *Comput. Phys. Commun.* **185**(6), 1747–1758 (2014).
- ³⁹K. Parlinski, Z. Q. Li, and Y. Kawazoe, *Phys. Rev. Lett.* **78**(21), 4063–4066 (1997).
- ⁴⁰T. Feng and X. Ruan, “Prediction of spectral phonon mean free path and thermal conductivity with applications to thermoelectrics and thermal management: A review” *J. Nanomater.* **2014**, 206370.
- ⁴¹M. Kitayama, K. Hirao, A. Tsuge, K. Watari, M. Toriyama, and S. Kanzaki, *J. Am. Ceram. Soc.* **83**(8), 1985–1992 (2004).
- ⁴²H. Liang, Y. Zeng, K. Zuo, Y. Xia, D. Yao, and J. Yin, *Ceram. Int.* **42**(14), 15679–15686 (2016).
- ⁴³Y. Duan, J. Zhang, X. Li, H. Bai, P. Sajgalik, and D. Jiang, *Int. J. Appl. Ceram. Technol.* **16**(4), 1399–1406 (2019).
- ⁴⁴J. S. Kang, M. Li, H. Wu, H. Nguyen, and Y. Hu, *Science* **361**(6402), 575–578 (2018).
- ⁴⁵S. Li, Q. Zheng, Y. Lv, X. Liu, X. Wang, P. Y. Huang, D. G. Cahill, and B. Lv, *Science* **361**(6402), 579–581 (2018).
- ⁴⁶F. Tian, B. Song, X. Chen, N. K. Ravichandran, Y. Lv, K. Chen, S. Sullivan, J. Kim, Y. Zhou, T. H. Liu, M. Goni, Z. Ding, J. Sun, G. A. G. U. Gamage, H. Sun, H. Ziyae, S. Huyan, L. Deng, J. Zhou, A. J. Schmidt, S. Chen, C. W. Chu, P. Y. Huang, D. Broido, L. Shi, G. Chen, and Z. Ren, *Science* **361**(6402), 582–585 (2018).
- ⁴⁷T. Feng, A. O’Hara, and S. T. Pantelides, *Nano Energy* **75**, 104916 (2020).
- ⁴⁸M. Simoncelli, N. Marzari, and F. Mauri, *Phys. Rev. X* **12**(4), 041011 (2022).
- ⁴⁹Z. Cheng, J. Liang, K. Kawamura, H. Zhou, H. Asamura, H. Uratani, J. Tiwari, S. Graham, Y. Ohno, Y. Nagai, T. Feng, N. Shigekawa, and D. G. Cahill, *Nat. Commun.* **13**(1), 7201 (2022).
- ⁵⁰Q. Zheng, C. Li, A. Rai, J. H. Leach, D. A. Broido, and D. G. Cahill, *Phys. Rev. Mater.* **3**(1), 014601 (2019).
- ⁵¹Z. Cheng, Y. R. Koh, A. Mamun, J. Shi, T. Bai, K. Huynh, L. Yates, Z. Liu, R. Li, E. Lee, M. E. Liao, Y. Wang, H. M. Yu, M. Kushimoto, T. Luo, M. S. Goorsky, P. E. Hopkins, H. Amano, A. Khan, and S. Graham, *Phys. Rev. Mater.* **4**(4), 044602 (2020).
- ⁵²R. J. Bruls, H. T. Hintzen, G. de With, and R. Metselaer, *J. Eur. Ceram. Soc.* **21**(3), 263–268 (2001).
- ⁵³R. Anzalone, M. Camarda, A. Canino, N. Piluso, F. La Via, and D. D’Arrigo, *Electrochem. Solid-State Lett.* **14**(4), H161 (2011).
- ⁵⁴J. Dai and Z. Tian, *Appl. Phys. Lett.* **118**(4), 041901 (2021).